Optical potentials for the elastic scattering of $^6Li + ^{12}C$, $^6Li + ^{16}O$, and $^7Li + ^{12}C$

M. F. Vineyard, J. Cook, K. W. Kemper, and M. N. Stephens
Department of Physics, Florida State University, Tallahassee, Florida 32306
(Received 14 May 1984)

New elastic scattering angular distributions extending over the large angular range 10°—170° c.m. are reported for $^6Li + ^{12}C$ at 24 and 30 MeV, $^6Li + ^{16}O$ at 25.7 MeV, and $^7Li + ^{12}C$ at 34 MeV. These data have been analyzed and are well described by the optical model using Woods-Saxon potentials, or by potentials with a double-folded real part. Using these and previously published data, average energy-dependent potentials have been obtained. Improved descriptions of the elastic scattering of $^6Li + ^{12}C$, $^6Li + ^{16}O$, and $^7Li + ^{12}C$ for energies from the Coulomb barrier up to 26 MeV/nucleon are obtained with these new average potentials compared with existing ones.

I. INTRODUCTION

New experimental data are reported for the elastic scattering of $^6Li + ^{12}C$ at 24 and 30 MeV, $^6Li + ^{16}O$ at 25.7 MeV, and $^7Li + ^{12}C$ at 34 MeV. The data extend over the large angular range of 10°—170° in the center-of-mass frame and are analyzed with the optical model using Woods-Saxon and double-folded potentials. The large-angle data provide a greater sensitivity to the potential than is possible with only forward angle data and aids in reducing the ambiguities in determining the optical potential.

The data measured here are used with previously published data to investigate the energy dependence of $^{6,7}Li$ scattering from ^{12}C and ^{16}O and to obtain energy dependent average optical potentials. Since previous studies[1–3] of energy dependence were published, more precise data, such as those reported here, have become available and the upper energy limit has been considerably extended. The old energy dependent optical potentials fail to reproduce the new data, particularly at large angles and high energies. There is therefore a need for improved average optical potentials for these light systems, preferably as consistent in form as possible with those already established[4] for $^{6,7}Li$ scattering on heavier targets.

In Sec. II we describe the experimental procedure used to measure the new data reported in this paper. The optical model analysis of these data is discussed in Sec. III A using Woods-Saxon potentials and in Sec. III B with double-folded potentials. The energy dependence of $^6Li + ^{12}C$, $^6Li + ^{16}O$, and $^7Li + ^{12}C$ elastic scattering is discussed in Sec. III C and average potentials are obtained. We discuss our results and present our conclusions in Sec. IV.

II. EXPERIMENTAL PROCEDURE

The elastic scattering angular distributions were taken in two separate pieces. The forward angle data were taken by scattering $^{6,7}Li$ from the appropriate target, while the large angle data were taken by detecting the $^{6,7}Li$ recoils arising from the scattering of ^{12}C and ^{16}O from $^{6,7}Li$ targets. The angular distributions were then pieced together with typically ten overlap points between the two sets of data.

The proton, $^{6,7}Li$, ^{12}C, and ^{16}O beams used in this scattering study were produced in an inverted sputter source[5] and accelerated to the desired energies by the Florida State super FN tandem Van de Graaff. Self-supporting natural carbon (98.9% ^{12}C) foils of thicknesses ranging from 100—300 $\mu g/cm^2$ and SiO_2 (99.7% ^{16}O) foils of thicknesses between 100—200 $\mu g/cm^2$ were used for the $^{6,7}Li + ^{12}C$ and $^6Li + ^{16}O$ measurements. The elastic scattering of ^6Li from free standing natural Si targets was measured at forward angles so that the Si yields could be removed from the combined Si+O peak to obtain the O yields. Natural Li targets (92.4% ^7Li) were used for the ^7Li recoil measurements and the ^6Li targets were enriched to 99.3%. The Li metal was deposited on Formvar backings and produced Li targets with thicknesses of 30—70 $\mu g/cm^2$. The Li targets were transferred under vacuum to avoid target deterioration from contact between the Li and the humid air in the laboratory.

Due to the copious α-particle production and the generally positive Q values for producing them, it was necessary to perform particle identification throughout the measurements. This was accomplished with many different combinations of silicon surface-barrier detectors used in $\Delta E \times E$ telescopes. A stationary single monitor counter was used during these measurements to check for carbon buildup on the targets and for inconsistencies in beam charge accumulation. Since Li has a relatively low melting point there is a danger of losing target material during the recoil Li measurements. Normally the yields obtained from the monitor detector can be used to check for target loss. However, in the present recoil study, the monitor yields were not as reliable as in the forward angle measurements because of the presence of contaminant peaks and a large continuum contribution to the scattering. Therefore the counter telescopes were returned to $\theta_{lab} = 15°$ and the recoil yield was compared with previous runs. The loss of target material was negligible.

Standard preamplifiers and amplifiers were used to process the detector signals which were then digitized and read by the on-line data acquisition computer. The $\Delta E \times E$ contours were displayed on a storage scope, gated

 ©1984 The American Physical Society

according to Z and M with a light pen and then sorted into linear energy spectra on line.

The absolute cross sections for the ^{6,7}Li+^{12}C, ^{16}O data were determined by first measuring the elastic scattering of 20 MeV ^{16}O ions from the ^{12}C and SiO_2 targets at $\theta_{lab}=15-20°$, where the scattering was found to be Rutherford and Mott, respectively. The Rutherford and Mott cross sections along with the elastic scattering yields were used to calculate the product of the detector solid angle and target thickness necessary to calculate the absolute cross section for the reaction of interest. The absolute uncertainty in the normalization of the cross sections is $\pm 7\%$ and arises from uncertainties in the normalization data runs from beam integration (3%), repeatability (3%), angle setting (2%), and counting statistics ($< 1\%$).

The product of the detector solid angle and target thickness ($Nd\Omega$) for the recoil ^{6}Li data was determined by measuring the elastic scattering of 6.868 MeV protons from ^{6}Li targets at $\theta_{lab}=95°$, where the cross section was previously determined by Bingham *et al.*[6] The obtained product $Nd\Omega$ was then used to calculate the absolute cross sections. Each data set for the ^{6}Li scattering had about ten overlap points between the set obtained by detecting the scattered ^{6}Li and that by detecting the recoil ^{6}Li. From these overlaps, it was found that the difference between the two absolute cross section measurements was $\pm 6\%$. For the ^{7}Li data, which were taken after the ^{6}Li data, the recoil cross sections were obtained from overlapping with the data obtained from the ^{7}Li scattering angular distribution.

Previous analyses[1–3] of the elastic scattering of ^{6}Li from light targets that have tried to develop global optical model potential sets in the energy region of 1–10 MeV/nucleon have been unable to describe the large angle rise in the elastic cross sections reported earlier by Chuev *et al.*[7] for ^{6}Li+^{12}C and ^{16}O. Generally, these large angle data have been omitted when the analyses have been published. One important goal of the present experiment was to determine if the previously reported large angle data was correct. The energy of 30 MeV, used in the ^{6}Li+^{12}C study, was chosen to be close to the energy of 30.6 MeV used by Chuev *et al.*,[7] so that any rapid changes in the shape of the angular distribution at large angles would be found. The present data agree very well in magnitude and location of the oscillations in the angular distribution. Yield curves at large angles for the ^{6}Li+^{12}C reaction previously reported by Fulton and Cormier[8] only show structure centered around 22.8 MeV FWHM of 800 keV. The present measurements also mapped out the forward angle oscillations, which had not been previously done. The present ^{6}Li+^{16}O data also confirm the rise in large angle cross section reported in Ref. 7 at 29.8 MeV, showing that this large angle rise is a general phenomena in light nuclei.

III. OPTICAL MODEL ANALYSIS

A. Woods-Saxon potentials

The ^{6}Li+^{12}C, ^{6}Li+^{16}O, and ^{7}Li+^{12}C elastic scattering data obtained from the experiments described in Sec. II were analyzed in terms of the optical model using Woods-Saxon potentials. Throughout this paper the heavy-ion radius convention [i.e., $R_x=r_x(A_p^{1/3}+A_t^{1/3})$] is used and a Coulomb potential for a point charge interacting with a uniformly charged sphere is included with the Coulomb radius parameter fixed at $r_C=1.25$ fm.

1. The ^{6}Li data

Initial fits to the 30 MeV ^{6}Li+^{12}C and the 25.7 MeV ^{6}Li+^{16}O data were performed using Woods-Saxon potentials starting with average potential parameters obtained from a preliminary study[9] of the energy dependences of the potentials for these systems. These parameters provided a reasonable description of the forward angle data, but did not fit the large angle data well. All the potential parameters were then searched on resulting in the parameter sets labeled III for the ^{12}C data and V for the ^{16}O data in Table I, and the fits shown as the full lines in Fig. 1. The fits to the data are quite good over the entire angular range for both systems and the final parameters are not drastically different from the average parameters used to start the searches. This demonstrates that the large angle data are extremely sensitive to the potentials.

Optical model searches were then performed on these two sets of data to investigate the possible existence of other parameter sets which fit the data. In these grid searches, the depth of the real potential was fixed at values of 50–300 MeV in 10 MeV intervals, and the real well geometry and imaginary radius parameters were

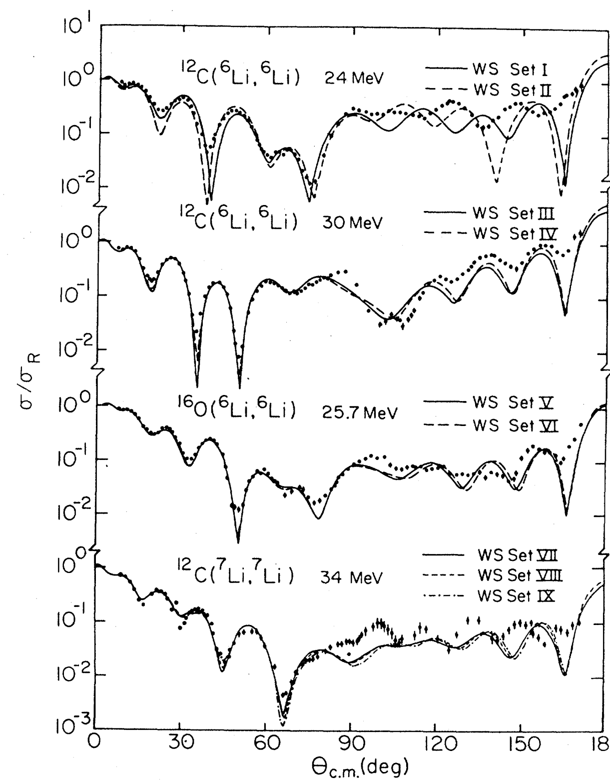

FIG. 1. Optical model fits to the ^{6}Li+^{12}C, ^{6}Li+^{16}O, and ^{7}Li+^{12}C elastic scattering data measured in this study. Woods-Saxon potentials were used with the parameters given in Table I.

TABLE I. Woods-Saxon optical model parameters. The nuclear potential has the form

$$U(r)=-V_0\Big/\left[1+\exp\left[\frac{r-R_R}{a_R}\right]\right]-iW_0\Big/\left[1+\exp\left[\frac{r-R_I}{a_I}\right]\right].$$

System	E (MeV)	Set	V_0 (MeV)	r_R[a] (fm)	a_R (fm)	W_0 (MeV)	r_I[a] (fm)	a_I (fm)
$^6Li+^{12}C$	24	I	129	0.84	0.70	8.10	1.22	0.67
		II	297	0.56	0.85	12.90	0.99	0.76
$^6Li+^{12}C$	30	III	186	0.63	0.83	7.74	1.26	0.69
		IV	244	0.65	0.75	9.95	1.16	0.78
$^6Li+^{16}O$	25.7	V	176	0.66	0.84	6.27	1.39	0.72
		VI	222	0.69	0.78	7.84	1.31	0.77
$^7Li+^{12}C$	34	VII	159	0.63	0.73	7.20	1.38	0.85
		VIII	223	0.63	0.68	8.64	1.31	0.92
		IX	290	0.64	0.64	10.71	1.22	0.97

[a] $R_x=r_x(A_p^{1/3}+A_t^{1/3})$.

fixed at the previously found values to limit the number of parameters varied. Only the imaginary potential depth and diffuseness were searched upon to fit the data, starting from the values of parameter sets III and V. Another minimum in the χ^2 space was found for both systems. The minimum occurred at $V_0=270$ MeV for the $^6Li+^{12}C$ data and at $V_0=230$ MeV for the $^6Li+^{16}O$ data. Starting with the parameters corresponding to these minima, all the potential parameters were then varied to fit the data, resulting in the parameter sets IV and VI of Table I and the fits shown as the dashed lines in Fig. 1. The fits are good over the whole angular range, and are of similar quality to those of parameter sets III and V.

Since two parameter sets which provide very similar fits to the data were found for both systems, the question arose as to whether the two sets are related in some way. In order to determine if sets III and IV for the 30 MeV $^6Li+^{12}C$ data are related through a discrete ambiguity in the depth of the real potential, searches were performed on V_0 and W_0, starting from the values of set III, while the geometry parameters (i.e., r_x and a_x) were fixed at the values of set IV. Similar searches were performed with parameter sets V and VI for the $^6Li+^{16}O$ data. The data for either system could not be fitted well with this procedure, indicating that neither pair of parameter sets are related through a discrete ambiguity. Since the diffuseness parameters are not the same, neither pair are members of the same Igo ambiguity[10] either. Searches were then performed to determine if they are members of different Igo ambiguities. In each of these searches, small changes were made in the radius and depth of one of the wells such that the Igo constant was preserved, and then the parameters of the other well were varied to fit the data. Good fits to the data could not be obtained for either system with this procedure; i.e., no Igo ambiguities were observed. A plot of the potentials showed that the two imaginary potentials for both systems crossed at two points, which is a general characteristic of potentials that are related through a $W_0R_I^n$ type of continuous ambiguity. However, it appears that the real potentials are not related in any way.

Calculations were then performed for the 24 MeV $^6Li+^{12}C$ data using the parameter sets III and IV obtained by fitting the 30 MeV $^6Li+^{12}C$ data. The forward angle ($\theta<90°$) data were fairly well described by both parameter sets, but the predictions were too low in magnitude and poorly matched in phase with the data at larger angles. Therefore, starting with the values of parameter sets III and IV, all the potential parameters were varied to fit the data, resulting in parameter sets I and II of Table I and the fits shown as the full and dashed lines, respectively, in Fig. 1. The fits to the 24 MeV data are quite inferior to the fits obtained for the 30 MeV data. This, and the fact that the forward angle data are fitted with the same potential at both energies, suggests that the large angle scattering may not be pure potential scattering. This feature of the scattering would not be apparent if only forward angle data had been taken.

There are two different philosophies which one can adopt in the case of the 24 MeV data. One could fit the forward angle data and assume that the large angle data have contributions other than those arising from pure potential scattering, or else one could fit the entire angular range and assume that a rapid energy dependence of the potential is present. It has previously been reported[1–3] that data for this system, over this energy range, could be described with a simple energy dependent potential. However, only forward angle data were analyzed in these studies and, even then, they reported only marginal success. In view of the present results, it is not surprising that the energy dependent potentials of Bindal *et al.*[2] and Poling *et al.*[3] do not provide an adequate fit to the present large angle data. The Poling potentials do, however, describe the forward angle data fairly well. The small angle fits to the $^6Li+^{12}C$ data with the Bindal potential are not as good as those with the Poling potential, but still describe the general features. This is one of the reasons we decided to reinvestigate the energy dependence of these light systems.

The 24 MeV data appear to be anomalous in that it was not possible to obtain a good fit to the data over the whole angular range with any of the potentials used in this analysis. An anomaly has previously been reported[11] for the scattering of polarized ^6Li from ^{12}C at 22.8 MeV in which it was found that the analyzing power changed rapidly as a function of energy. Fulton and Cormier[8] conducted a detailed search for anomalous effects in ^{6}Li+^{12}C elastic and inelastic scattering over the energy range $E_{lab}=20$—36 MeV. Excitation functions for the ground state and the first excited state (4.44 MeV) of ^{12}C were measured at 10 angles in the range $\theta_{c.m.}=40°$—160°. The data indicate the occurrence of a single resonantlike structure of width $\Gamma \approx 800$ keV at $E_{lab}=22.8$ MeV, which shows up at intermediate angles in the elastic channel and at back angles in the inelastic channel. Predictions of their elastic scattering excitation functions at three angles using potentials III and IV are shown in Fig. 2. The agreement is not very good at the larger angles, but this may be because the angles chosen are at minima in the angular distributions where sensitivity to the potential is at its greatest.

2. *The ^{7}Li data*

The 34 MeV ^{7}Li+^{12}C data were now fitted with Woods-Saxon potentials starting with set III obtained for the 30 MeV ^{6}Li+^{12}C data. A comparison of the two experimental angular distributions reveals a very different behavior in the angular region 60°—90°, and also at the largest angles, where the cross sections are an order of magnitude smaller for ^{7}Li than for ^{6}Li. This indicates that different potentials are required to fit the two projectiles. All the potential parameters were searched on, resulting in potential set VIII and the fit shown as the dashed line in Fig. 1. The fit is satisfactory for forward angles ($\theta < 80°$), but does not describe the data particularly well at larger angles. A grid search on the depth of the real potential was then carried out and additional minima in the χ^2 space were found for $V_0=160$ MeV and 280 MeV. The potential parameters corresponding to these two minima were then varied to fit the data, resulting in parameter sets VII and IX of Table I and the fits shown as the full and dot-dashed lines in Fig. 1. The fits are almost identical to that of parameter set VIII. Within the limitation of Woods-Saxon potentials we were unable to find any other potential which would result in an improved description of the large angle data. The real potentials of parameter sets VII, VIII, and IX do not appear to be related, while the imaginary potentials belong to a $W_0R_I^n$ type of continuous ambiguity.

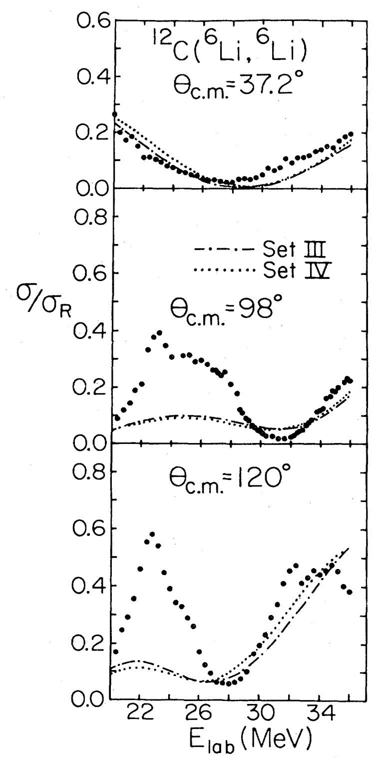

FIG. 2. Predictions of the elastic scattering excitation function for ^{6}Li+^{12}C using Woods-Saxon potentials III and IV from Table I. The experimental data are from Ref. 8.

B. Double-folded potentials

In addition to Woods-Saxon real potentials, double-folded real potentials were used in an optical model analysis of the elastic scattering data measured here. The real double-folded potentials were obtained with the computer code DFPOT (Ref. 12) by convoluting the $M3Y$ effective nucleon-nucleon interaction[13] with the projectile and target ground state densities as discussed by Satchler and Love.[14]

The particular form of the $M3Y$ interaction used included a component to account for single-nucleon knockout exchange and had the explicit form

$$v(r)=7999\frac{e^{-4r}}{4r}-2134\frac{e^{-2.5r}}{2.5r}-390\delta(\vec{r}) \ . \tag{1}$$

The ^{6}Li density was obtained from the measured charge density of Suelzle *et al.*[15] by unfolding the proton charge distribution and assuming the neutron and proton densities to be identical. An LS coupling model[16] was used for ^{7}Li. The density consisted of spherical and quadrupole parts to enable an investigation of the effect of ground state quadrupole reorientation in the projectile on the elastic scattering angular distributions. The ^{7}Li ground state density was therefore

$$\rho(r)=(0.319+0.0232r^2)e^{-0.334r^2} -0.419r^2e^{-0.334r^2}Y_{20}(\hat{r}) \ . \tag{2}$$

Here the vector $\vec{r}$ refers to the body-fixed axes and the quadrupole density is normalized to an intrinsic quadrupole moment $Q_{20}=22.5\ e\,\mathrm{fm}^2$ assuming $J^\pi=\frac{3}{2}^-$, $K=\frac{1}{2}$, and an experimental quadrupole moment $Q_2=-4.5$ $e\,\mathrm{fm}^2$ (Ref. 17) for ^{7}Li. Harmonic oscillator densities were used for the target nuclei, and are given by

$$\rho(r)=(0.173+0.0647r^2)e^{-0.352r^2} \tag{3}$$

for ^{12}C, and

$$\rho(r)=(0.141+0.0647r^2)e^{-0.298r^2} \tag{4}$$

for ^{16}O. The proton charge distribution was also unfolded from these last two densities.

The conventional Woods-Saxon form was used for the imaginary part of the optical potential, and the usual Coulomb potential with the radius parameter fixed at $r_C = 1.25$ fm was included. Optical model searches were then performed. At this stage only the spherical part of the ^{7}Li density was used. The real double-folded potentials were multiplied by a renormalization factor N. Initially, the renormalization factor was fixed at $N=1.0$ and the imaginary potential parameters were extensively searched upon to fit the data. As usual, good fits to the data could not be obtained with this procedure. The best fits obtained with $N=1.0$ are shown as the dashed lines in Fig. 3. The normalization factors were then searched upon, along with the imaginary potential parameters, resulting in the parameter sets of Table II and the fits shown as the full lines in Fig. 3. The fits to the 30 MeV ^{6}Li+^{12}C data and the ^{6}Li+^{16}O data are good over the whole angular range, and are of very similar quality to those obtained with Woods-Saxon real potentials. However, as was found with Woods-Saxon real potentials, it was not possible to obtain a good fit to the 24 MeV ^{6}Li+^{12}C data over the entire angular range. A one shot calculation with the 30 MeV ^{6}Li+^{12}C folded potential described the forward angle ($\theta \leq 90°$) 24 MeV data well, and, with some adjustment of the imaginary potential, a very good fit to the forward angle data was obtained. Even after allowing N to vary it was not possible to obtain good fits to the ^{7}Li+^{12}C data, the phasing at forward angles and the oscillatory structure from intermediate to large angles being incorrect.

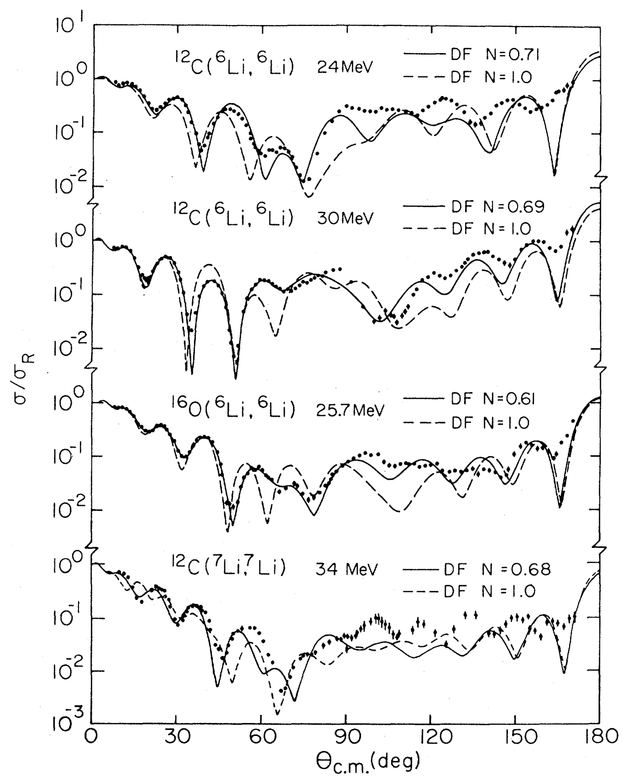

FIG. 3. Optical model fits to the ^{6}Li+^{12}C, ^{6}Li+^{16}O, and ^{7}Li+^{12}C elastic scattering data measured in this study. The potential consisted of a double-folded real potential multiplied by the renormalization factor N and a Woods-Saxon imaginary part. The potential parameters are given in Table II.

TABLE II. Double-folded optical model parameters. The nuclear potential has the form

$$U(r)=NV_F(r)-iW_0 \Big/ \left[1+\exp\left[\frac{r-R_I}{a_I}\right]\right],$$

where $V_F(r)$ is the calculated double-folded potential.

System	E (MeV)	N	W_0 (MeV)	r_I[a] (fm)	a_I (fm)
^{6}Li+^{12}C	24	0.71	6.77	1.34	0.59
^{6}Li+^{12}C	30	0.69	8.65	1.17	0.82
^{6}Li+^{16}O	25.7	0.61	6.62	1.35	0.80
^{7}Li+^{12}C	34	0.68	10.67	1.21	1.14

[a] $R_x = r_x(A_p^{1/3}+A_t^{1/3})$.

Calculations were then made using the optical model code HERMES (Ref. 18) for ^{7}Li+^{12}C, including the quadrupole part of the ^{7}Li density. It has previously been reported[19] that, at low energies, inclusion of this part removes the need for any renormalization of the real folded potential, but a null effect was found[20] at higher energies. Searches were made starting both with $N=1.0$ and with the parameters of Table II. A quadrupole imaginary form factor was included, being of a derivative Woods-Saxon—type, with a deformation length of 3.4 fm. Even after extensive searching it was not possible to obtain good fits to the data, either with $N=1.0$ or $N \approx 0.7$. In particular the oscillatory structure was damped far too much by inclusion of the quadrupole term. It must therefore be concluded that inclusion of the quadrupole part of the ^{7}Li density does not resolve the problem of fitting the present ^{7}Li+^{12}C data or of why $N \approx 0.7$.

Optical model calculations were then performed for the ^{6}Li+^{12}C data using real double-folded potentials generated with microscopic ^{12}C densities to investigate the sensitivity of the scattering to the shape of the target density. The microscopic densities used were those of Kamimura[21] and Bassel *et al.*[22] which describe electron scattering data well. These calculations resulted in fits and potential parameters essentially identical to those in Fig. 3 and Table II.

The normalization factors of $N \approx 0.7$ found here for the ^{6}Li and ^{7}Li folded potentials are consistent with those found in other studies of ^{6}Li and ^{7}Li scattering. The reduction of N below unity is generally thought to be due to projectile breakup effects. Including coupling to the 3^+ 2.18 MeV unbound state in ^{6}Li, through which sequential breakup may proceed, is found[23] to reduce the discrepancy. It is hoped that when the full continuum breakup cross section is included in coupled channels calculations, maybe along the lines of the work of Sakuragi *et al.*,[24] that the need for any renormalization may be removed.

C. Energy dependent average potentials

Our general philosophy for obtaining average potentials is enunciated in two previous papers.[4,25] Those papers investigated the energy dependence and obtained average potentials for ^{6,7}Li scattering over the energy range 13—156 MeV for targets ranging from ^{24}Mg to ^{208}Pb. We did not find any necessity for including energy dependence in these potentials; however, subsequent data extending to large angles for ^{6}Li scattering from ^{28}Si (Ref. 26) and ^{40}Ca (Ref. 27) at energies around 30 MeV required an imaginary potential much weaker and with a larger radial extent than higher energy data. Optical potentials for scattering from lighter target nuclei are more likely to show fluctuations in the parameters due to nuclear structure and channel coupling effects, and thus in this paper we aim to obtain average potentials for each of the ^{6}Li+^{12}C, ^{6}Li+^{16}O, and ^{7}Li+^{12}C systems separately.

Average energy-dependent optical potentials have already been obtained for these projectile-target combinations. Poling *et al.*[1] considered ^{6,7}Li+^{12}C scattering for energies from 4.5 to 13 MeV. Four parameter searches (V,W,R,a) were conducted with a surface imaginary potential. A large number of different potentials were obtained, with the imaginary well depth W increasing linearly with energy. Poling *et al.*[3] later included ^{6}Li+^{16}O data for energies from 4.5 to 50.6 MeV and extended the energy range of ^{6}Li+^{12}C and ^{7}Li+^{12}C to 63 and 36 MeV, respectively. They obtained six-parameter average potentials with either the real well depth V and/or the surface imaginary well depth W linearly dependent on the bombarding energy. Bindal *et al.*[2] obtained six-parameter fits to 20—63 MeV ^{6}Li+^{12}C data with V linearly decreasing and the volume imaginary well depth increasing with energy.

Since these studies additional data are available. The energy range has been considerably extended and high quality large angle data, as presented in this paper, exist. The previously determined average potentials fail when applied to these new data. It is therefore an opportune moment to reexamine these systems in detail and obtain average potentials which are consistent in general form with those we have found[4] for heavier targets.

In our present calculations we have, in addition to the new data measured here, employed previously published data for ^{6}Li+^{12}C over the energy range from 4.5 to 156 MeV,[3,11,28–35] ^{6}Li+^{16}O from 4.5 to 50.6 MeV,[3,7,11,30,31,36] and ^{7}Li+^{12}C from 4.5 to 88.8 MeV.[3,30,37–40] As far as possible we have obtained data in tabulated numerical form, but had to resort to tracing some of the older data from published figures. An optical model search was performed separately for each data set, starting from the data and potentials found in Sec. III A, and going up and down in energy from these using the potentials found at each energy as the starting parameters for the next energy. After this was completed, the optical-model parameters for each projectile-target combination were plotted versus energy to establish parameter trends to be used in obtaining average energy-dependent potentials. An extended version of the code GENOA (Ref. 41) was used to simultaneously fit all the data for a certain projectile-target combination to find average potentials. Each angular distribution was weighted to give approximately the same χ^2 per point when a good fit was obtained. The results for each system are discussed separately below.

1. ^{6}*Li*+^{12}*C*

The fits at individual energies revealed that both the real and imaginary diffusenesses, a_R and a_I, remained rather constant over the energy range 4.5—156 MeV, while W_0 increased and r_I decreased linearly with energy. The real well depth V_0 decreased with energy and the radius of the real potential well r_R was fairly constant, except for the 22.8 and 24 MeV data where V_0 exhibited a sudden decrease and r_R a sudden increase followed by a return to the general trend. Since there appears to be a resonance in this energy region (see Sec. II A 1), it is not unexpected to find rapid changes in the optical model parameters for these energies. To try to account for this in the average energy dependent potential we included in V_0 and r_R a narrow Gaussian term centered on 22.8 MeV. The average potential finally obtained is listed in Table III and fits using it are shown in Fig. 4. The overall quality of the fits is very good, and in particular the description of the large angle data is much better than that of the potential of Poling *et al.*[3] (It should be noted that in Fig. 4 of Ref. 3 the 30.6 MeV data are truncated at $\theta=130°$ and the unshown data for $\theta>130°$ are poorly described by their potential.) There are some features of the data, however, which are not reproduced. The magnitude of the data at 22.8 MeV and the large angle behavior at 22.8 and 24 MeV are not described well. This is probably related to the occurrence of a resonance in this energy region which was not accounted for completely by the inclusion of a Gaussian "glitch" in the potential parameters. The

TABLE III. Energy dependent optical model parameter. The form of the nuclear potential is the same as in Table I. In the table below $X=\exp[-(E-23/2)^2]$.

System	E (MeV)	V_0 (MeV)	r_R[a] (fm)	a_R (fm)	W_0 (MeV)	r_I[a] (fm)	a_I (fm)	r_C[a] (fm)
^{6}Li+^{12}C	4.5—156	$174-20X$	$0.69+0.08X$	0.79	$1.03+0.26E$	$1.36-0.0021E$	0.62	1.25
^{6}Li+^{16}O	4.5—50.6	159	0.71	0.83	$2.14+0.19E$	$1.46-0.0047E$	0.81	1.25
^{7}Li+^{12}C	4.5—88.8	167	0.60	0.80	9.57	1.31	0.72	1.25

[a] $R_x=r_x(A_p^{1/3}+A_t^{1/3})$.

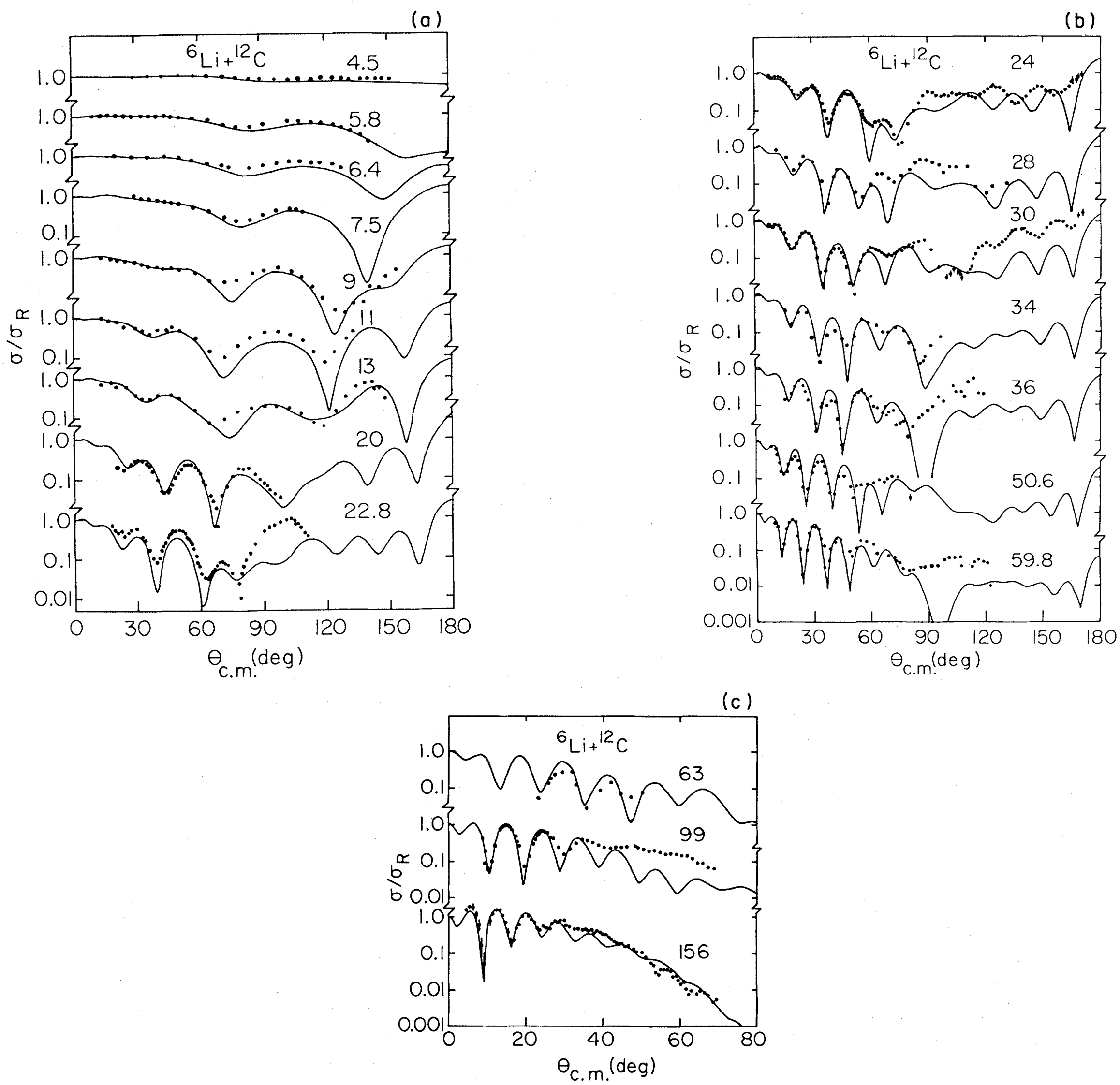

FIG. 4. Optical model fits to ^{6}Li+^{12}C elastic scattering data using the average energy dependent potential of Table III. Each curve is labeled by the projectile energy in MeV.

calculations at 36 and 59.8 MeV show deep minima for $\theta \approx 90°$, whereas the measured cross sections are fairly constant. The experimental data at these energies may be individually fitted reasonably well with the potential for the 36 MeV data not seeming to deviate from the average trend, but that for the 59.8 MeV data having a weaker real part and a stronger imaginary part. This indicates that there may be some rapid energy dependence in the potential around 60 MeV, although the angular region around 90° is very sensitive to the interference of waves scattered into the forward and backward hemispheres so no strong claim is made to this. At 99 MeV (where in this and other studies it is found necessary to multiply the experimental data by 1.6) the average potential fails to reproduce the structureless falloff in the cross sections for $\theta \approx 40°$, although it does very much better at 156 MeV. This indicates a change in the nature of the optical potential in this energy region.

2. $^6Li+^{16}O$

The fits to ^{6}Li+^{16}O data at individual energies exhibited a linear dependence of W_0 and r_R on energy, with no discernible energy dependence in the remainder of the parameters. The final energy-dependent parameters are listed in Table III, resulting in the fits shown in Fig. 5. The description of the data is very good over the whole energy range at all angles. In particular, the large angle data at 25.7 and 29.8 MeV are well described both in phase and magnitude, whereas the potential of Poling *et al.*[3] underpredicts the large angle data at 29.8 MeV by a factor of about 4.

3. $^7Li+^{12}C$

Individual energy fits to ^{7}Li+^{12}C data failed to reveal any systematic energy dependence in the ^{7}Li+^{12}C optical model parameters except perhaps for a small decrease of

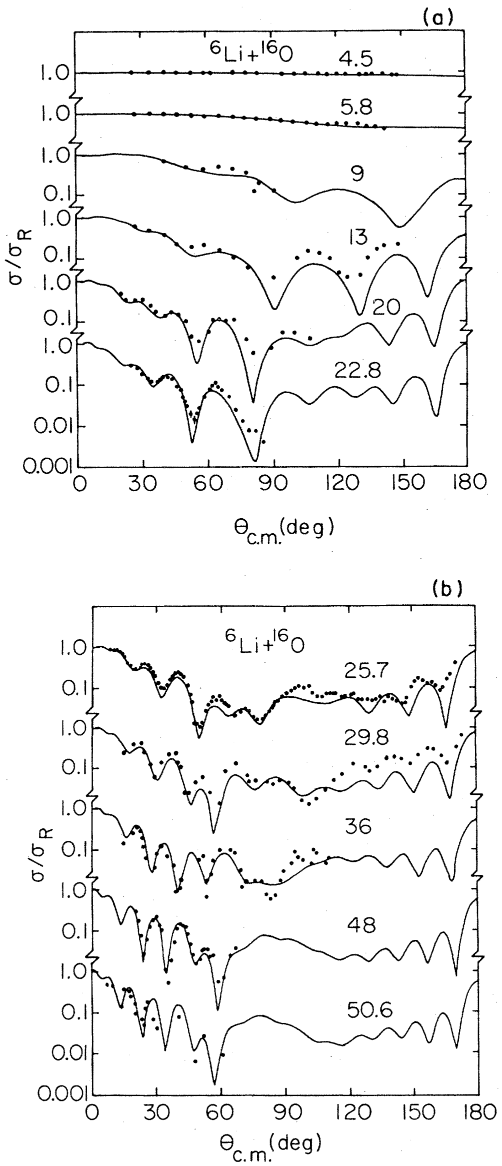

FIG. 5. Optical model fits to ^{6}Li+^{16}O elastic scattering data using the average energy dependent potential of Table III. Each curve is labeled by the projectile energy in MeV.

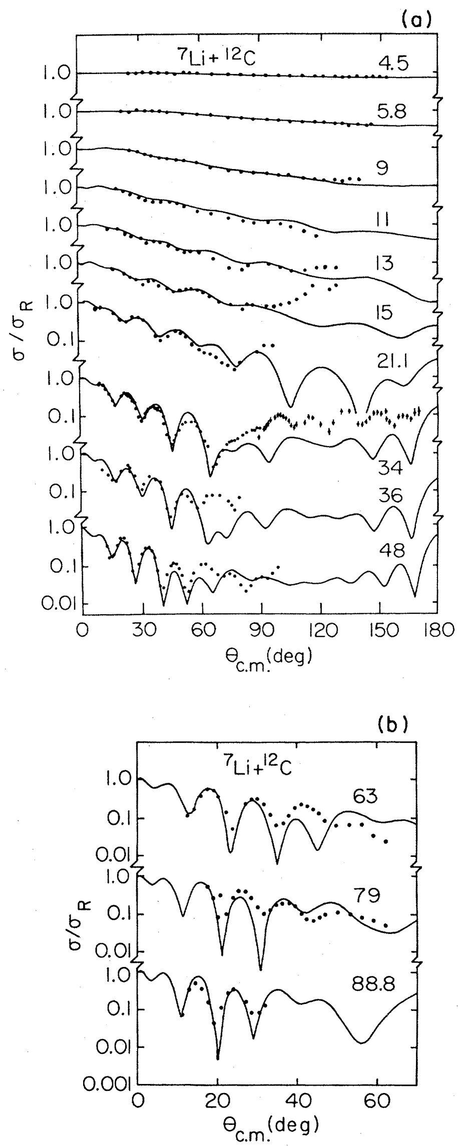

FIG. 6. Optical model fits to ^{7}Li+^{12}C elastic scattering data using the average potential of Table III. Each curve is labeled by the projectile energy in MeV.

V_0 with increasing energy. Good fits could be obtained with an average potential which contained no energy dependence in any of the parameters. This is given in Table III with the fits resulting from it shown in Fig. 6. The data are fairly well described at all energies. However, there are some features which are not reproduced. The data at 15 MeV show an increase in cross section for $\theta > 100°$ which cannot be reproduced with any Woods-Saxon potential we have tried. The agreement between the data and the calculations at 36 and 48 MeV for $\theta = 60°-90°$ is not excellent, nor is it for $\theta > 35°$ at 63 MeV. For energies above 60 MeV reorientation in the ^{7}Li ground state has some effect on the angular distribution, and this is why the data at these energies do not show such pronounced minima as the calculated angular distributions do. This may be compensated for by an increase in the strength of the imaginary potential so that the minima become filled in, but this is an incorrect procedure since there is a well understood physical process behind their origin. Unfortunately, we do not have the capability of including the quadrupole reorientation term in our global calculations, but only for one energy at a time.

IV. DISCUSSION AND CONCLUSIONS

New elastic scattering data have been measured over the large angular range of 10–170° c.m. for ^{6}Li+^{12}C at

24 and 30 MeV, $^6Li+^{16}O$ at 25.7 MeV, and $^7Li+^{12}C$ at 34 MeV. These data have been fitted with the optical model using Woods-Saxon and double-folded potentials. Several different Woods-Saxon potentials were found to fit each angular distribution well, although the fits to the 24 MeV $^6Li+^{12}C$ data were of inferior quality to the others. This could be related to the occurrence of a resonant-like structure around $E_{lab}=22.8$ MeV in $^6Li+^{12}C$ excitation function data. The double-folded potentials were calculated by convoluting the $M3Y$ effective nucleon-nucleon interaction with the ground state densities of the projectile and target nuclei. The potentials needed to be reduced in strength by about 30% in order to reproduce the data. Similar quality fits, except for $^7Li+^{12}C$, were then obtained to those using Woods-Saxon potentials.

Energy dependent average potentials of the Woods-Saxon form have been obtained for $^6Li+^{12}C$, $^6Li+^{16}O$, and $^7Li+^{12}C$ from energies around the Coulomb barrier to 156, 63, and 89 MeV, respectively. The parameters are either constant or vary linearly with energy, except for $^6Li+^{12}C$ around 22–24 MeV where the real potential depth and radius parameter exhibit an abrupt deviation from the general trend. The average parameters account well for the overall behavior of the data, and the fits at large angles are much improved over those obtained from previous universal studies. Only small departures from the average parameters are required to obtain fits at each energy as good as those which can be acquired by fitting each angular distribution separately. However, even those individual fits are unable to precisely describe the data at some energies. This may indicate the presence of scattering processes other than pure shape elastic scattering.

This work was supported in part by the National Science Foundation.

[1]J. E. Poling, E. Norbeck, and R. R. Carlson, Phys. Rev. C **5**, 1819 (1972).
[2]P. K. Bindal, K. Nagatani, M. J. Schneider, and P. D. Bond, Phys. Rev. C **9**, 2154 (1974).
[3]J. E. Poling, E. Norbeck, and R. R. Carlson, Phys. Rev. C **13**, 648 (1976).
[4]J. Cook, Nucl. Phys. **A388**, 153 (1982).
[5]K. R. Chapman, Nucl. Instrum. Methods **124**, 299 (1975).
[6]H. G. Bingham, A. R. Zander, K. W. Kemper, and N. R. Fletcher, Nucl. Phys. **A173**, 265 (1971).
[7]V. I. Chuev, V. V. Davydov, B. G. Novatskii, A. A. Oglobin, S. B. Sakuta, and D. N. Stepanov, J. Phys. (Paris) **36**, C6-161 (1971).
[8]B. R. Fulton and T. M. Cormier, Phys. Lett. **97B**, 209 (1980).
[9]J. Cook (unpublished).
[10]G. Igo, Phys. Rev. Lett. **1**, 72 (1958); Phys. Rev. **115**, 1665 (1959).
[11]W. Weiss, P. Egelhof, K. D. Hildenbrand, D. Kassen, M. Makowska-Rzeszutko, D. Fick, H. Ebinhaus, E. Steffens, A. Amakawa, and K.-I. Kubo, Phys. Lett. **61B**, 237 (1976).
[12]J. Cook, Comput. Phys. Commun. **25**, 125 (1982).
[13]G. Bertsch, J. Borysowicz, H. McManus, and W. G. Love, Nucl. Phys. **A284**, 399 (1977).
[14]G. R. Satchler and W. G. Love, Phys. Rep. **55**, 183 (1979).
[15]L. R. Suelzle, M. Y. Yearian, and H. Crannell, Phys. Rev. **162**, 992 (1967).
[16]F. Petrovich and D. Stanley, Nucl. Phys. **A275**, 487 (1977).
[17]G. J. C. van Niftrik, L. Lapikas, H. de Vries, and G. Box, Nucl. Phys. **A174**, 173 (1971), and references therein. The value of Q_2 used is that determined from nuclear beam spectroscopy. Values of $Q_2 \approx -3.7\ e\ \mathrm{fm}^2$ are found from electron scattering.
[18]J. Cook, Comput. Phys. Commun. **31**, 363 (1984).
[19]V. Hnizdo, K. W. Kemper, and J. Szymakowski, Phys. Rev. Lett. **46**, 590 (1981).
[20]J. Cook, M. F. Vineyard, K. W. Kemper, and V. Hnizdo, Phys. Rev. C **27**, 1536 (1983).
[21]M. Kamimura, Nucl. Phys. **A351**, 456 (1981).
[22]R. H. Bassel, B. A. Brown, R. Lindsay, and N. Rowley, J. Phys. G **8**, 1215 (1982).
[23]M. F. Vineyard, K. W. Kemper, and J. Cook, Phys. Lett (in press).
[24]Y. Sakuragi, M. Yahiro, and M. Kamimura, Prog. Theor. Phys. **68**, 322 (1982); **70**, 1047 (1983).
[25]J. Cook, Nucl. Phys. **A375**, 238 (1982).
[26]M. F. Vineyard, J. Cook, and K. W. Kemper, Nucl. Phys. **A405**, 429 (1983).
[27]J. Cook, K. W. Kemper, and M. F. Vineyard, Phys. Rev. C **26**, 486 (1982).
[28]K. Bethge, K. Meier-Ewert, and K. O. Pfeiffer, Z. Phys. **208**, 486 (1968).
[29]G. Bassani, N. Saunier, B. M. Traore, J. Raynal, A. Foti, and G. Pappalardo, Nucl. Phys. **A189**, 353 (1972).
[30]P. Schumacher, N. Ueta, H. H. Duhm, K.-I. Kubo, and W. J. Klages, Nucl. Phys. **A212**, 573 (1973).
[31]L. T. Chua, F. D. Becchetti, J. Jänecke, and F. Milder, Nucl. Phys. **A273**, 243 (1976).
[32]H. G. Bingham, M. L. Halbert, D. C. Hensley, E. Newman, K. W. Kemper, and L. A. Charlton, Phys. Rev. C **11**, 1913 (1975).
[33]R. W. Ollerhead, C. Chasman, and D. A. Bromley, Phys. Rev. **134**, B74 (1964).
[34]D. P. Stanley, F. Petrovich, and P. Schwandt, Phys. Rev. C **22**, 1357 (1980).
[35]J. Cook, H. J. Gils, H. Rebel, Z. Majka, and H. Klewe-Nebenius, Nucl. Phys. **A388**, 173 (1982).
[36]J. Cook, L. C. Dennis, K. W. Kemper, T. R. Ophel, A. F. Zeller, C. F. Maguire, and Z. Kui, Nucl. Phys. **A415**, 114 (1984).
[37]K. A. Weber, K. Meier-Ewert, H. Schmidt-Böcking, and K. Bethge, Nucl. Phys. **A186**, 145 (1972).
[38]A. F. Zeller, K. W. Kemper, D. C. Weisser, T. R. Ophel, D. F. Hebbard, and A. Johnston, Nucl. Phys. **A323**, 477 (1979).
[39]A. F. Zeller, Y. W. Lui, R. E. Tribble, and D. M. Tanner, Phys. Rev. C **22**, 1534 (1980).
[40]H. S. Bradlow, W. D. M. Rae, P. S. Fisher, N. S. Godwin, G. Proudfoot, and D. Sinclair, Nucl. Phys. **A314**, 207 (1979).
[41]F. G. Perey (unpublished).